

NATURE AND ORIGIN OF MINERAL COATINGS ON VOLCANIC ROCKS
OF THE BLACK MOUNTAIN, STONEWALL MOUNTAIN, AND KANE
SPRINGS WASH VOLCANIC CENTERS, SOUTHERN NEVADA

Dr. James V. Taranik, Principal Investigator
Dr. Donald C. Noble, Co-Principal Investigator
Dr. Liang C. Hsu, Co-Investigator
David M. Spatz, Co-Investigator

Mackay School of Mines
Department of Geological Sciences
University of Nevada, Reno
Reno, Nevada 89557

July, 1987
Semiannual Progress Report for Period January, 1987 -
July, 1987

Contract Number NAS5-28765

(NASA-CR-181209) NATURE AND ORIGIN OF	N87-26473
MINERAL COATINGS ON VOLCANIC ROCKS OF THE	
BLACK MOUNTAIN, STONEWALL MOUNTAIN AND KANE	
SPRINGS WASH VOLCANIC CENTERS, SOUTHERN	Unclas
NEVADA Semiannual Progress (Nevada Univ.)	41 G3/46 0087894

Prepared for
The National Aeronautics and Space Administration
Goddard Space Flight Center
Greenbelt, Maryland 20771

TABLE OF CONTENTS

	Page
Abstract	1
Work Accomplished	2
Activities Anticipated	2
Introduction	3
Study Sites	3
Method of Investigation	4
Imagery Characteristics	6
Mineral Coatings	10
Origin of Coatings	23
Geochemical Models	30
Influence of Coatings on Imagery	32
Conclusions	36
References	37

LIST OF FIGURES

1. Location map	3
2. TM image of Stonewall	8
3. TM image of Stonewall	8
4. TM image of Black Mtn	8
5. TM image of Black Mtn	8
6. Photomicrograph of coating	14
7. Outcrop of trachyte	14
8. Density slice of coating	15
9. SEM photo of coating	15
10. SEM coating composition	17
11. SEM coating map	18
12. SEM line scan of coating	22
13. SEM line scan of coating	22
14. XRD curves of coatings	24
15. IR spectrophotometry curves	25
16. Eh-pH diagram of Mn and Fe	27
17. Thickness vs absorption	34
18. Beckman lab spectra	35

LIST OF TABLES

Table 1. SEM compositions	19
Table 2. ICP analyses	21

MINERAL COATINGS ON VOLCANIC ROCKS
OF THE BASIN AND RANGE PROVINCE - NATURE, ORIGIN,
DISTRIBUTION, AND IMPORTANCE TO LANDSAT TM IMAGERY

D.M.Spatz, J.V.Taranik, L.C.Hsu

ABSTRACT

Mineral coatings, including desert varnish on volcanic rocks of the semi-arid Basin and Range province are composed of amorphous, translucent films of Fe, Mn, Si, and Al rich compounds. Coatings are chiefly thin films that impregnate intergranularly to depths of about 0.1-0.3mm, rarely deeper. Varnish accumulations of greater than 5 micrometers are greatly subordinated by much thinner films, are discontinuous, and tend to concentrate in recesses in rock surfaces. Where thick accumulations were observed, Mn is concentrated at the coating air interface and within coating interlayers. Fe is more continuous throughout coatings but is often concentrated at the base of coatings at the rock interface. Fe/Mn ratios and total combined Fe-Mn are higher in mafic rock coatings relative to more felsic units, suggesting a genetic relationship with underlying host rocks.

Source considerations for Mn indicate that sufficient background levels of Mn are present in the substrate of most rocks investigated to provide all the Mn in the coatings from only a few mm depths. A weathering cortex forms on all rock assemblages studied. The cortex is distinguished most readily in the more porous tuffs by an enrichment in Ca and Mg and a calcareous cement. A possible leaching origin for coatings from underlying host rocks by a solution front model similar to that which forms caliche in aridic soils is discussed.

Comparative lab spectra and Thematic Mapper imagery investigations indicate coatings are relatively absorbant below about 0.7 to 1.3 micrometers, depending on mafic affinity of the sample, but less absorbant than mafic host rocks at higher wavelengths. In some cases the divergence is lost at higher wavelengths (bands 5 and 7). Distribution of significant varnish accumulations - over 5 micrometer thicknesses - is sparse and localized, occuring chiefly in surface recesses. These relationships result in dominance of lithologic spectral responses in the longer wavelenth bands. The spectral contribution of vegetation, like mineral coatings, appears in some instances subordinate to lithologic responses in longer wavelength bands as well.

WORK ACCOMPLISHED SINCE LAST REPORTING PERIOD

Efforts over the past 6 months concentrated on the analytical portion of the contract, although some additional imagery processing activity continued, as well as further field work. Analytical methods and accomplishments are detailed in a following section.

In summary, 16 coating sections and subsurface interiors were probed by SEM; 20 samples were scanned by infrared spectrometry; 10 samples were scanned for visible-near IR spectra; induction coupling plasma analyses were collected on 34 samples; 2 desert varnish surfaces were investigated by optical density slice imagery; a few XRD analyses were conducted in addition to the 50 reported on last period; thin section observation continued; and imagery processing focused on classification techniques.

In late May, approximately 10 field days were spent at the Stonewall and Black Mountain study sites conducting more detailed mapping and observation based on imagery results and collecting spectra with the school's new Collins Field Spectrometer. Approximately 100 spectral analyses were collected and are currently being processed.

ACTIVITIES ANTICIPATED FOR NEXT REPORTING PERIOD

Efforts over the next 6 months will concentrate on processing and analyzing field spectra; correlating ground spectra with TM pixel values; documenting, by charts and graphs, reflectance characteristics of rock types and coatings; more direct analyses of imagery/mineral coating relationships; drafting geologic and special imagery feature maps; drafting exhibits depicting coating origin model; and additional SEM and other analytical activities.

INTRODUCTION

Continuing the Mackay School of Mines' NASA supported Landsat Thematic Mapper (TM) project, this past semester focused on the nature, composition, and origin of secondary mineral coatings on volcanic rocks at the 3 project sites and varnish influence on TM imagery. Analytical methods, described herein, involved SEM, ICP, IR spectra, and Beckman IR/near-IR spectra. Image processing techniques were described in a previous report. Most XRD work was conducted in the Fall of 1986.

This report is preliminary. Final conclusions should await final collection of data sometime in 1988.

STUDY SITES

The three study sites selected for investigation (Figure 1) provide superior settings in terms of exposure, preservation, diversity, and a pre-existing data base collected principally by previous researchers at Mackay. Each study site is approximately 9 x 9 miles (14.5 x 14.5 kilometers) and encompassed within a 512 x 512 pixel Landsat 5 TM subscene. Each site centers on or straddles a well defined youthful caldera structure with discrete ash flow tuff deposits and associated lavas and subvolcanic intrusive bodies. More detailed geologic and individual unit descriptions were presented in a previous report.



FIGURE 1. LOCATION OF LANDSAT TM TEST SITES

These volcanic centers represent distinctive peralkaline magmatic systems active between about 6.5 m.y.a. (Stonewall) to 15 m.y.a. (Kane Springs). Each center was source for multiple ash flow sheets that extend from the calderas up to 30 km distally. Some of these major pyroclastic deposits are distinct from each other chemically, mostly in regard to iron content, both divalent and trivalent, the latter resulting from auto-oxidation processes during deposition and cooling. The ash flows are rhyolites to comenditic rhyolites, and at Black Mountain the final ash flow extrusion, the Gold Flat Member, is a rare pantellerite (greater than 4% iron). Devitrification, vapor-phase alteration, and welding history also vary from unit to unit and within units. Intracaldera lavas include basalts, trachyandesites, mafic trachytes, and rhyolite lavas and flow domes.

The climate within the Basin and Range province of southern Nevada is semi-arid. Rainfall averages 4-8 inches annually. Vegetative cover at the three sites is nominal to sparse and includes scrub evergreen trees and shrubs at some of the higher elevations and mesa tops, sage brush, atroplex, box brush, foxtail grass, cheat grass, and succulents (mostly at Kane Springs Wash), including cholla and yucca. Elevations range from 6500 to 3000 feet at Kane Springs Wash. Relief is much less at the other 2 sites: 600 at Stonewall, 1500 at Black Mountain.

METHOD OF INVESTIGATION

Analytical investigations of coatings began in the Fall of 1986. At that time over 50 thin sections were studied to varying degrees of detail and 52 X-ray diffraction (XRD) analyses completed. This past winter (1987) efforts concentrated on SEM studies. In addition, further XRD and thin section investigations were conducted, IR spectrometry performed, Inductively coupled plasma (ICP) analyses run, Beckman lab spectra collected (visible and near-IR), and density slice gray level measurements made from coating photographs. The suite of samples selected for these applications represent select, major volcanic units present at each of the 3 study sites as well as the diverse coating types observed. Detail on the specific methods employed follow.

THIN SECTION PETROGRAPHY. Over 70 thin sections have been prepared. Each is cut perpendicular to the rock surface, exhibiting surface coatings, and extending down into the host rock. In this perspective, boundaries between surface coatings and underlying host

can be observed and relationships noted. Each section was ground to 3 micrometer thicknesses by a Nevada Bureau of Mines technician with explicit instructions to maintain section edges and edge thicknesses. Petrographic investigations are being conducted on a standard binocular petrographic microscope.

XRD. Coating material from surface chips and subsurface zones of 58 representative rock units was extracted for XRD analysis. The technique employed involved briskly and lightly vibrating fine powder size material from the rock surface with an electric scribe with a carbide steel tip. Some of the extraction was accomplished under a Baush and Lomb zoom binocular scope. Although the scribe has both diamond and tungsten carbide tips available, these harder points tend to drill beneath the surface coatings into underlying fresher rock. Still, much of the coating compositions collected in this manner contain primary rock constituents. To improve sample purity, powders were screened to 100 mesh to exclude coarser particles likely to involve underlying primary minerals, then ground in an agate mortar prior to mounting on a glass slide for X-ray analysis. (Greater than 90% by volume of the particles extracted from the rocks were less than 100 mesh, 0.147mm). We believe that little material beyond this thickness (0.2mm) contaminates the samples.

All samples were X-rayed on one of Mackay's Philips Norelco XRD instruments and 2 theta measurements calibrated to a known quartz standard. Samples were saved in numbered glass vials.

SEM. Scanning electron microscope studies were conducted on a JEOL T300SEM, equiped with an energy dispersive X-ray system EDXS, at the U.S. Bureau of Mines in Reno. Sixteen samples were prepared either by polished sections encapsulated in epoxy or by polished thin sections from which cover glasses were removed. Each sample was scanned and compositional probes tabulated for coatings, weathering rinds, subsurface weathering bands, fresh rock interiors, and individual mineral grains. Textures were observed in secondary X-ray mode and photographed. Coating encrustations were photographed and compositional line scans run. The unit is equiped with a Peak Instruments wavelength spectrometer for carbon analysis. The SEM imagery was processed on a Princeton Gamma Tech microcomputer and data saved on disc.

I.R. SPECTROPHOTOMETER. Twenty samples including coating powders, subsurface weathering bands, rock interiors, and 2 opal and manganese oxide knowns were scanned on the University of Nevada's Perkin-Elmer

model 599 Infra red spectrophotometer. Samples were encapsulated in a KBr pellet and compared to a pure pellet. A 3 minute scan time was used from 2.5 to 50 micrometers (4000-200 wavenumber) and graphed on a log scale.

DENSITY SLICE. Gray level density slice measurements of 2 photographs of ash flow tuff surfaces hosting moderately mature coatings were collected on a Dapple Systems optical image analysis system at the U.S. Bureau of Mines. The unit utilized a Panasomic movie camera and an Apple IIe image processing peripheral. Gray level histograms were computed at a scale of 0-255. Gray levels thought visually to represent coated surfaces were compared to gray levels of fresh rock surfaces exposed within the photographic frame.

VISIBLE LAB SPECTRA. Visible and near-IR spectral measurements, comparing coated to noncoated surfaces, were plotted on the Jet Propulsion Lab's Beckman UV5240 UV-Visible-NIR spectrophotometer. The instrument uses a diffraction grating as its dispersion element, a tungsten source lamp and a halogen reference tube. Ten samples, representing some of the more variable rock types at the study sites were scanned between 0.4 and 2.5 micrometers and percent reflectance measured.

ICP. Inductive coupling plasma analyses of coatings, weathering rinds, rock interiors, and one carefully prepared subsurface weathering band, were analyzed for 10 major elements, H₂O, CO₂, and S. Analyses were performed by Chemex Laboratories in B.C., Canada. Weathered cortex samples were carefully prepared by removing weathered surfaces with coatings with a trim saw. Coatings were excavated from rock surfaces by grinding wheel or electric scribe. ICP is an especially effective type of atomic spectroscopy in which samples are "atomized" by a super heated argon gas plasma and emission spectra analyzed for absorption peaks representative of the various elements present. Twenty-five analyses, including weathering rinds and rock interiors, from 12 rock samples were reported. Nine coating samples were analyzed as well.

IMAGERY CHARACTERISTICS

Late summer to fall Landsat 5 TM scenes were read onto disk and all processing conducted on the Mackay School of Mines' VAX 11/780 based ESL compact interactive digital image manipulation system (IDIMS).

A multivariate statistical evaluation for each scene was conducted with IDIMS function ISOCLS. A mean and standard deviation for each band and covariance and

correlation matrices were computed to aid band selection. The principle components (PC) transformation utilizes variance and covariance statistics. Resulting eigenvalues give a measure of the relative contribution of individual PC's to the variance and individual bands to individual PC's. Standard imagery processing techniques (Taranik, 1978) were employed. Single band images are presented in Figures 2, 3, 4, and 5.

STONEWALL MOUNTAIN AREA

SPEARHEAD TUFF. The Spearhead Tuff exhibits little spectral variation throughout the visible and near-IR. It is dark in all TM bands. Reflectivity decreases slightly and the unit darkens subtly in band 5 relative to other cover in the scene. Darker trends tend to increase the tonal contrast somewhat in 5/7 images. Intensity decreases slightly in the 3/1 ratio image; increases slightly in 5/1 images. In individual principle component images, the unit is brightest in PC3 with high brightness also in PC2 and PC4. ISH computation on bands 3-5-7 result in indistinct low contrast tones over the unit in the saturation and hue modes, darker though in the intensity image.

CIVET CAT CANYON TUFF. Reflectance over Civet Cat is low in bands 1, 2, and 3 and high in bands 4, 5, and 7, increasingly so in the later 3 relative to other cover in the scene. These spectral relationships cause subdued tones in 3/1 and 5/7 ratio images, but strikingly bright contrast in the 5/1 ratio image. There is a low intensity but high saturation and hue response for the unit in ISH computations with bands 3-5-7. On ISH images with bands 1-2-4 the unit shows low values in intensity and hue, high values in saturation, but low contrast in all three modes. Civet Cat is strikingly bright in PC2 images, growing somewhat less so in PC's 3 and 4.

FELSIC TUFF AND PORPHYRY. The unit exhibits high reflectivity in all bands with diminishing intensity in longer wavelength bands 5 and 7. Several exposures are quite bright in 5/7 ratio images. The unit contrasts markedly with other formations in most color composite images. On the ISH computations, bands 3-5-7, the unit is bright in saturation and intensity, light to medium gray in hue. In 1-2-4 ISH renditions the deposit is quite dark in hue and saturation, light in the intensity mode. These felsic rocks respond with bright intensity in PC1, dark and indistinct in PC2.

BLACK MOUNTAIN CALDERA

Imagery over the Black Mountain study area differs from Stonewall due both to more diverse vegetation and



FIGURE 2. Landsat 5 TM band 1 (stretched) image of the Stonewall Mountain area. Image is approximately 10 km square. R-rhyolite/latite tuffs and flows, S-Stonewall Flat Tuff, G-quartzite gravels, B-basalt.



FIGURE 3. Landsat 5 TM principle components (first PC) image of the Stonewall Mountain site. Image is approximately 10 km square. Legend is under Figure 2.



FIGURE 4. Landsat 5 TM band 2 (stretched) image of the Black Mountain caldera. Image is approximately 10 km square.



FIGURE 5. Landsat 5 TM bands 3, 5, and 7 saturation image (stretched) of the Black Mountain caldera. Image is approximately 10 km square. G-Gold Flat Tuff, T-Older Thirsty Canyon Tuff, H-Trachyte of Hidden Cliff, L-Labyrinth Canyon Tuff, F-pre-Black Mountain felsic rocks.

ORIGINAL PAGE IS
OF POOR QUALITY.

lithologies. The 4/3 ratio image highlights zones with relatively heavy growth. This image is matched very closely by the PC3 image which also presents vegetation in strikingly bright contrast.

GOLD FLAT TUFF. The Gold Flat Tuff is an unusual rock petrochemically and is distinctive spectrally as well. Reflectance increases as wavelength increases to brightest in band 7. The unusually high reflectance in band 7 relative to other scene cover gives rise to a strikingly bright turquoise blue hue in the 3-5-7 composite. Gold Flat Tuff is bright in PC1, very dark and anomalous in PC2, and dark as well in PC3 except over its northern exposures where it is masked by the bright response of vegetation. The unit is intensely bright in saturation and hue images with ISH transformation on bands 3-5-7. It is light purple in the 1-4-Hue (bands 3-5-7), blue where vegetation includes golden grasses and scattered low juniper.

TRACHYTE OF HIDDEN CLIFF. Mafic trachyte forms the central volcanic edifice and is very dark in all bands except 4 and 5. Spectral response appears to be influenced by vegetation, in this case, golden cheat grasses and lichen. The unit is very bright in the 5/7 and 4/3 images in a striped pattern that apparently follows drainages with relatively dense vegetation. In individual PC's the deposit is quite dark in the first PC, very light due to vegetative interference in the third. In the ISH transform of bands 3-5-7, the unit is very dark in intensity and hue, medium gray and indistinct in saturation.

LABYRINTH CANYON TUFF. The Labyrinth Canyon ash flow tuff, a distal facies of Spearhead Tuff, is spectrally similar to Gold Flat Tuff. It tends to be moderately to only slightly bright in bands 1-3, quite bright in bands 4 and 5, somewhat less so in band 7. It is slightly less reflectant in band 7 than Gold Flat which aids its discrimination in false color composite images which take this relationship into account. It is bright in the 3/1 image, possibly due to its orangy buff color, and medium gray with 5/7 ratios. The unit is bright in PC1, dark in PC2. It appears masked by the bright vegetative response of cheat grass in PC3. Saturation and hue images of bands 3-5-7 give the unit a bright signature.

MINERAL COATINGS IN DESERT ENVIRONMENTS

Early attempts to describe mineral coatings in desert environments (desert varnish) in a comprehensive fashion were published by White (1924), Laudermilk (1931), and Engel and Sharp (1958). A more quantitative approach to the study of coatings began in the mid-1970's and numerous workers have published their results since. Dorn and Oberlander (1981) in a fairly lengthy treatise on the topic do an excellent job of summarizing work on coatings up to that time.

Desert varnish is usually defined as the arid secondary phase of the weathered surface of rocks in arid to semi-arid environments. Taylor-George, et.al. (1983) define desert varnish as a coating of ferromanganese oxide and clay. Perry and Adams (1978) found that varnishes they studied consisted of alternating bands with variable detrital minerals of clay, feldspar, quartz, and hematite. According to Dorn and Oberlander (1981), desert varnish averages 10-30 microns thick. To most field geologists desert varnish is that conspicuous dark rusty brown to shiny black stain that commonly coats prominent desert bluffs. Iron and manganese oxides are the distinctive components.

The term coating is used here, rather than desert varnish. Mineral coating is herein defined as any inorganic secondary mantle or weathering product that occurs on the outer surface of rocks to an indefinite depth and conceals to some degree fresh, primary lithologies. Coatings could conceivably consist of secondary replacement products developed by hydration, hydrolysis, or metasomatic ionic exchanges with primary rock minerals, or precipitated or attached exogenous material. The composition of any inorganics present is not to be treated except inasmuch as they serve as catalysts to help control the chemical environment of coating formation.

For purposes of remote sensing, we are concerned with the entire surface of any rock exposure, which may include both true desert varnish, subvarnish alteration zones, and relatively fresh rock with or without an incipient phase of alteration. Any given scene typically contains a combination of rock surface types, depending on host composition, textures, and topographic occurrence. Previous workers who have attempted to establish absolutes with regard to ultimate source of varnish constituents diverge on conclusion. Engle and Sharp (1958) concluded that the

components of desert varnish are derived from the underlying host rock, whereas Dorn and Oberlander (1981) state flatly that the constituents of "all rock varnishes" are derived from sources external to the host rock. Source of varnish constituents and relative proportions of exposure of varnish to underlying rock bear significantly on remote sensing interpretations.

Varnish and probably all coatings seem to require considerable time to form. Hunt (1961) cites archeological evidence to establish a threshold of about 2000 years for noticeable development. Exceptions may occur, however, and Engle and Sharp (1958) note one locality with noticeable varnish development over a 25 year period. Coatings tend to be amorphous and have a dark brown streak. Hardness of typical coatings on rocks of the Mojave Desert were measured at 4.5-5 (Laudermilk, 1931). Coatings adhere to their host tenaciously. They are insoluble in water, but readily soluble in hot, dilute hydrochloric acid. Varnishes are described to overly light "limonitic" staining and light clay alteration.

Coating morphology varies from paint-thin films to lamellar successions of light and dark layers. Borns, et.al. (1980) observed microorganisms, either mold or fungus, with a scanning electron microscope (SEM) in lamellar type coatings. Staley, et.al. (1982) describe abundant microcolonial structures of lichen, algae, and fungi on desert rock surfaces from the southwest U.S. They point out that lichen and algae can derive their nutrients from their host, but fungi require an external source and speculate that that external source is probably wind blown dust. By analysis with SEM-EDAX (energy dispersive X-ray system), Taylor-George, et.al. (1983) discovered Fe, Al, and Si, three of the characteristic elements of varnish, in fungi on rock surfaces from the Sonoran Desert. They also identified manganese oxidizing bacteria in the varnish as well. Perry and Adams (1978) found cyclic manganese deposition in lamellar coatings.

Comprehensive chemical data on varnishes were published by Engel and Sharp (1958). Their wet chemical determinations from rocks of southern California established O, H, Si, Al, Fe, and Mn as the chief elemental components. Spectrographic analyses discovered that Ti, Ba, and Sr were present in unusually high concentrations followed by other trace metals whose relative amounts seemed dependent on local geology. Compositional analysis of coatings by SEM reveals an MnO₂ concentration of up to 25% by weight (Hooke, et.al., 1969; Allen, 1978; and Perry and Adams, 1978). This anomalously high amount is difficult to reconcile given background MnO₂ concentrations in rock,

soil, and dust on the order of 0.1%. Biological concentration is usually evoked to account for the MnO_2 . SEM analyses by Hooke, et.al. (1969) on varnishes from Death Valley revealed an outer layer rich in Fe and Mn, with Mn/Fe increasing toward the surface, and an inner zone enriched in SiO_2 and Al_2O_3 . The total thickness of the varnish was 20-50 micrometers. Optical and Sem analysis by Allen (1978) on varnishes from Sonoran Desert rocks indicated high concentrations of Mg as well as Mn and Fe. This metal rich layer is approximately 20 micrometers thick and consists of a "clay-like" matrix separated from the host rock by a 1mm thick weathered cortex. The cortex is composed of unoriented microcrystals probably derived from the host. These bands, also described by Engel and Sharp (1958) are attributed to the weathering process. Allen concluded the source for the metals is external to the host.

The significant contribution of both SiO_2 and Al_2O_3 to the chemical composition of coatings is attributed by Allen (1978) and Potter and Rossman (1977, 1979) to clay minerals. Potter and Rossman feel the Fe and Mn oxides of varnish are in intimate association with mixed layer illite-montmorillonite clay minerals. They still surmise, however, that the clay minerals are probably externally derived by wind. Farr and Adams (1984) and Curtiss, et.al. (1985) discovered short lived hydrous alumina-silica coating up to 5 micrometers thick on very fresh basalts in semiarid parts of Hawaii.

Recent investigations stress a possible biological origin for some desert varnishes (Krumbein and Jens, 1981; Dorn and Oberlander, 1981; Taylor-George, et.al., 1983; Staley, et.al., 1983). It was noted above that some workers propose that all elemental constituents in varnish are derived externally. Neutron activation analyses by Knauss and Ku (1980) for trace elements and radioisotopes indicated that both U and associated Th in desert varnishes from the Colorado Plateau in Utah were derived from sources external to the host rocks. In a contrary view, Glasby, et.al. (1981) hold that varnish on dolerite from Antarctica is derived by leaching of elements from the substrate. They arrive at this conclusion by comparing analyses of whole rock with varnish compositions, the later of which is not enriched in manganese as is the case with varnishes from the southwest U.S.

NATURE OF COATINGS IN THE PROJECT AREAS

Coatings on the volcanic rocks at Stonewall Mountain, Black Mountain, and Kane Springs Wash are

typical of weathered surfaces on rocks throughout the semi-arid West and Southwest, U.S. Descriptions of coatings in general and details of analytical investigations by other workers in similar environments were presented above. This section describes the nature, distribution, and compositional characteristics of the coatings we have investigated to date. Analytical methods have also been described in an earlier section.

DISTRIBUTION

Coatings vary with underlying host rock in a manner generally congruous with host petrochemistry, degree of welding, devitrification, hyalinity, porosity, and other textural and physiochemical properties. Coatings may vary consistently enough from one formation to another to differentiate units in the field, inferentially. The basic observation and assumption is that darker, thicker coatings represent the more mature accumulations, which correlate well with relatively dense insoluble rocks, resistant to mechanical degradation.

Desert varnishes at these study sites tend to be thin, translucent films that resemble a stain at the rock surface (Figure 6). The coating penetrates into the substrate up to about 0.5mm, intergranularly between grains. Coated surfaces are underlain by a weathering rind that exfoliates eventually from the outcrop, exposing a nonvarnished surface that in time will develop varnish, and which in time will be removed on another exfoliation surface. Thus any given outcrop of dense rock, like densely welded ash flows, basalt, and rhyolite flow domes that host mature coatings will also exhibit surfaces with varying degrees of desert varnish (Figure 7). Even within a zone of quite dense, mature varnish, fresh mineral grains are randomly exposed.

The case hardened weathering rind that varnishes tend to ride are typically .5-20mm thick. The underlying substrate on the ash flow tuffs is usually a cream, buff, or orangy buff variably calcareous zone, stained lightly in places with limonitic iron oxides. The zone is largely absent in most lavas and vitric tuffs, particularly the basalts and mafic trachytes. Thin section observation revealed that one subsurface zone comprised of a very fine grained mesh of secondary sericite, possibly derived from late stage cooling and possibly associated with "cooling rinds", apparently rare in the study areas.

A density slice of a black and white photograph of densely welded Civet Cat Canyon Tuff (Figure 8) shows

ORIGINAL PAGE IS
OF POOR QUALITY

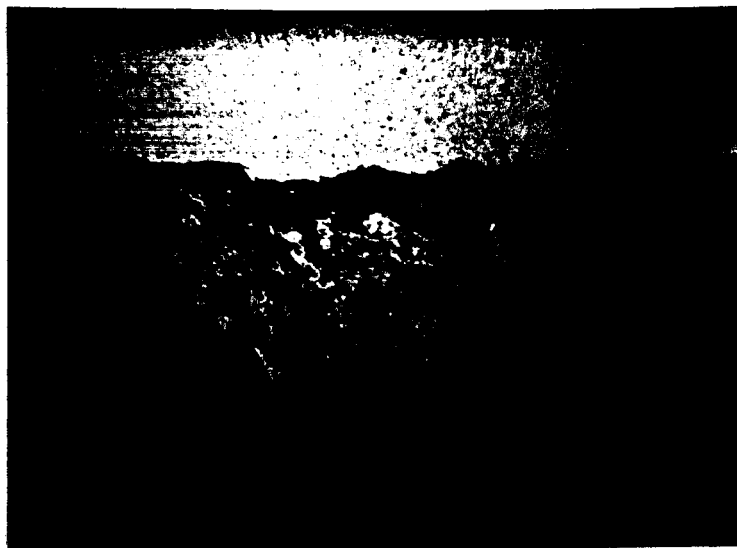


FIGURE 6. Photomicrograph of ash flow tuff, showing a typical section of surface coating. Original magnification - 2.5x.



FIGURE 7. Field photograph over outcrop of mafic trachyte of the Black Mountain caldera, showing mineral coating distribution.

CIVET CAT CANYON TUFF

F-Fresh, Uncoated



COATED ROCK SURFACE

GRAY LEVEL DENSITY SLICE

FIGURE 8. Gray level density slice of a photograph of moderately varnished surface of Civet Cat Canyon Tuff. The gray level separation was selected visually to distinguish fresh rock exposure (F) from darker mineral coatings.

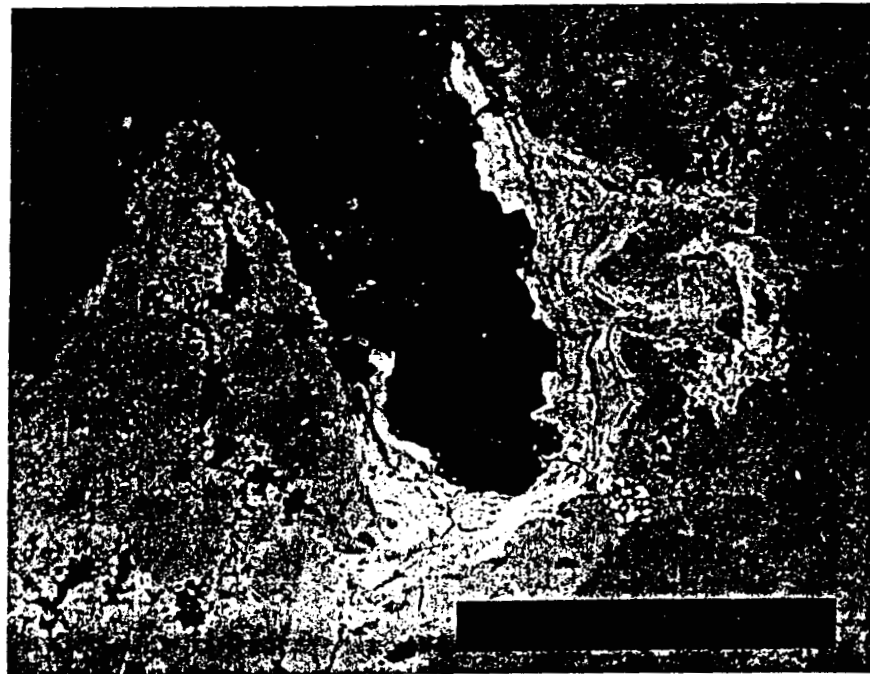


FIGURE 9. SEM backscatter image of section across rhyolite surface from Stonewall Mountain, showing laminar desert varnish (light tone) in rock recess. 1 inch=80 micrometers.

the distribution of coatings within a surface exhibiting moderately mature coating development. In this example, a fresh rock exposure is used for calibration, and surfaces that are darker and known from visual observation to be coated are density sliced to show coating distribution - in this case, 37%. Bear in mind that this represents a zone of outcrop with relatively mature coating development and that a significant proportion of any sizeable outcrop contains uncoated surfaces.

Thin section and SEM observation reveal that rock surfaces with varnish build-up or layering is relatively minor, most of the coating consisting of a thin, penetrative film. Where coating accumulations and layering has been observed, it tends to favor small recessed in the rock surface (Figure 9). Thicknesses observed vary from less than 5 to about 50 micrometers. There seems to be some tendency for coatings to accumulate at surface intersections with thin glassy zones in the tuffs, even though glassy units in general do not exhibit mature coatings due to their nonresistant nature.

CHEMICAL COMPOSITION

Coating compositions in general are consistent in major element composition from unit to unit. SEM probes indicate coatings are composed chiefly of Fe, Mn, Si, and Al (Figures 10 and 11, Tables 1 and 2), Fe and Mn accounting for roughly 50-60%. The coatings contain some Ti, Ca, K, and Na, and Ca tends to be depleted relative to the alkalis, relative to the underlying host rock. The coatings and the underlying weathering rind both contain higher H₂O and S than the host rock.

The Fe/Mn ratio in the coatings varies. The most consistent relationship seems to be that Mn forms laminar concentrations (Figure 12) and has been observed at a peak in concentration at the outer surface of the coating (Figure 13). Fe tends to remain fairly consistent throughout the coating (Figures 12 and 13), and the Fe/Mn ratio usually increases toward the lower part of the coating (Figure 11). Where coatings penetrate into the rock below encrusted layers, the Fe/Mn ratio is usually higher.

PHASES

Thin section observation, X-ray diffraction analyses, SEM probes, and IR spectrophotometry indicate that the coatings are composed of amorphous compounds. XRD curves are dominated by primary mineral phases, underlying and intermixed with the coatings. Elevation in the XRD intensity over a broad area at a 2 theta

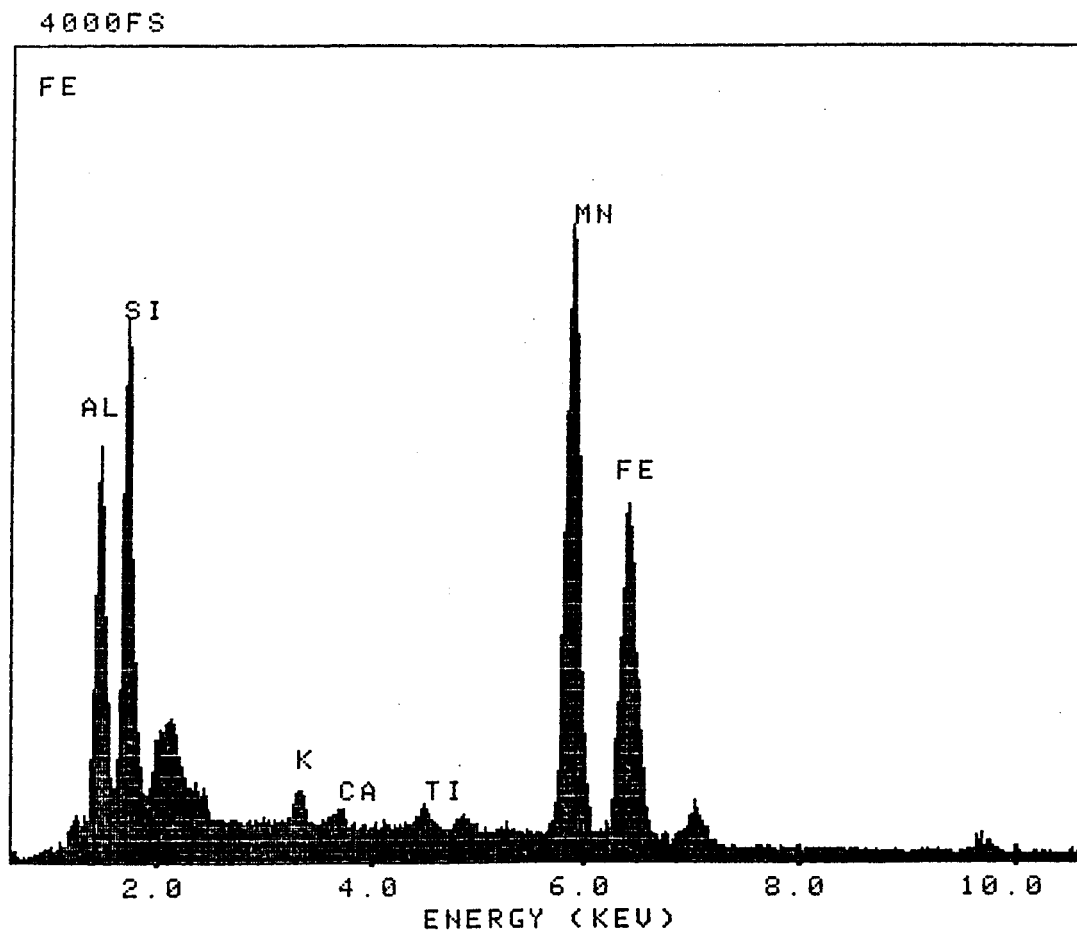


FIGURE 10 SEM compositional plot of coating on Civet Cat Canyon Tuff from Stonewall Mountain, showing high Fe, Mn, Si, Al, & Mn/Fe content.



FIGURE 11 SEM compositional map of coating on ash flow tuff. Higher intensities and concentrations are colored orange for Fe, dark green for Mn, red for K, and dark blue for Al. Fe is concentrated toward the coating base. Mn shows vague lamination.

ORIGINAL PAGE IS
OF POOR QUALITY

SEM COMPOSITIONAL PROBES

KS-21 BASALT SW-20 ASH FLOW BM-11 MAFIC TRACHYTE

ELEMENT	WEIGHT %
Na	1.33
Al	8.44
Si	8.53
K	0.69
Ca	0.42
Ti	1.31
Mn	21.79
Fe	24.78
O	32.72
TOTAL	100.00

COATING

ELEMENT	WEIGHT %
Na	2.20
Al	15.94
Si	18.24
K	0.83
Ca	0.59
Ti	2.18
Mn	28.13
Fe	31.88
O	100.00
TOTAL	100.00

ROCK BELOW

COATING

ELEMENT	WEIGHT %
Na	3.68
Al	9.96
Si	31.88
K	4.63
Ca	1.61
Mn	0.89
Fe	0.78
O	48.86
TOTAL	100.00

ROCK

INTERIOR

ELEMENT	WEIGHT %
Na	0.26
Al	0.88
Si	6.47
K	35.41
Ca	5.32
Ti	0.95
Mn	0.25
Fe	0.23
O	2.49
TOTAL	100.00

MINERAL

COMPOSITION

ELEMENT	WEIGHT %
Na	0.35
Al	0.88
Si	12.23
K	75.76
Ca	6.41
Ti	1.33
Mn	0.42
Fe	0.29
O	3.28
TOTAL	100.00

OLIVINE

BM-11

AEGERINE

BM-59

ELEMENT	WEIGHT %
Na	8.94
Al	15.38
Si	0.29
Ca	1.48
Mn	38.84
Fe	35.87
O	100.00
TOTAL	100.00

ELEMENT	WEIGHT %
Na	7.79
Al	0.00
Si	24.51
K	0.24
Ca	0.16
Ti	0.78
Mn	0.94
Fe	25.24
O	39.52
TOTAL	100.00

ELEMENT	WEIGHT %
Na	18.51
Al	0.00
Si	52.43
K	0.29
Ca	0.23
Ti	1.17
Mn	1.21
Fe	32.47
O	100.00
TOTAL	100.00

ORIGINAL PAGE IS
OF POOR QUALITY

CERTIFICATE OF ANALYSIS A8711598

Chemex Labs Inc.

Analytical Chemists - Geochemists - Registered Analysts
155 GLENDALE AVE., UNIT 7, SPARKS,
NEVADA, U.S.A. 89431
PHONE (702) 336-3393

To: SPATZ, MR. DAVID

100 - 3485 LAKESIDE DR.
RENO, NEVADA
89509

Project:
Comments:

Page No. 11
Tot. Pages: 1

Date: 23-MAR-87
Invoice #: A8711598
P.O. #: 214,254

CO2 % Inorg	S % (Leco)	FeO %	+H2O %	-H2O %	SiO2 %	Al2O3 %	Fe2O3 %	MgO %	CaO %	Na2O %	K2O %	TiO2 %	P2O5 %	MnO %	LOI %
BH-13 weathering rind	0.88	0.033	4.21	0.27	0.37	57.42	17.17	7.39	2.11	5.18	4.91	3.99	1.060	0.72	0.17
BH-13 rock interior	1.09	0.005	3.59	0.20	0.32	58.21	17.37	7.38	1.96	5.28	4.97	4.06	1.070	0.78	1.50
BH-46 rock interior	0.39	0.008	0.57	0.25	0.45	71.72	12.52	3.78	0.77	0.85	3.02	4.55	0.220	0.13	1.29
BH-46 weathering rind	2.07	0.004	0.35	0.25	0.35	67.88	14.15	3.72	0.26	3.41	5.37	4.85	0.250	0.15	2.75
BH-60 weathering rind	0.46	0.050	0.94	0.29	0.54	70.15	11.37	6.51	0.55	1.19	4.76	4.41	0.310	0.21	1.87
BH-60 rock interior	0.47	< 0.001	0.93	0.20	0.25	70.43	11.92	6.54	0.25	0.88	5.00	4.75	0.310	0.17	1.10
KS-10 weathering rind	1.44	< 0.001	0.31	0.10	0.21	74.44	13.15	1.08	0.18	2.34	4.31	4.45	0.030	0.11	0.03
KS-10 rock interior	0.39	< 0.001	0.28	0.08	0.22	76.43	13.38	1.16	0.12	0.94	4.29	4.42	0.040	0.09	0.03
KS-18 weathering rind	3.12	0.023	0.17	0.39	0.40	72.76	10.27	2.11	0.60	4.80	3.21	3.97	0.150	0.17	0.05
KS-18 rock interior	0.14	< 0.001	0.31	0.26	0.25	78.40	11.84	2.10	0.14	0.66	3.67	4.53	0.140	0.25	0.04
KS-21 weathering rind	0.07	0.002	6.48	0.28	0.25	48.60	16.39	12.10	6.50	8.65	3.07	1.24	2.000	0.73	0.16
KS-21 rock interior	0.07	< 0.001	5.98	0.26	0.19	54.39	17.15	9.18	4.46	7.71	3.09	1.94	1.480	0.47	0.12
KS-24 weathering rind	0.14	< 0.001	0.65	0.35	0.33	69.39	15.08	4.86	0.61	0.82	4.75	5.32	0.520	0.25	0.14
KS-24 rock interior	< 0.01	0.047	0.70	0.24	0.30	67.46	15.16	5.13	0.45	1.31	5.03	5.10	0.650	0.29	0.13
KS-26 weathering rind	0.07	0.003	0.47	0.43	0.30	69.20	14.82	4.62	0.16	0.62	4.76	5.20	0.440	0.21	0.07
KS-26 rock interior	0.07	< 0.001	0.33	0.33	0.31	69.38	15.12	5.14	0.14	0.77	4.90	5.38	0.500	0.20	0.05
SW-10 weathering rind	< 0.01	< 0.001	0.19	0.47	0.18	73.00	14.62	3.58	0.05	0.18	1.12	9.92	0.130	0.15	< 0.01
SW-10 rock interior	< 0.01	0.037	0.23	0.34	0.20	75.47	13.07	0.77	0.07	0.32	0.99	9.31	0.300	0.12	0.01
SW-20 weathering rind	2.18	0.008	0.25	0.24	0.30	66.76	14.77	2.83	0.47	4.02	4.26	5.48	0.360	0.22	0.10
SW-20 rock interior	0.63	< 0.001	0.12	0.52	0.37	70.87	14.41	2.71	1.00	1.87	4.20	5.31	0.330	0.22	0.10
SW-27 weathering rind	3.39	0.033	0.11	0.46	0.36	70.50	10.61	2.01	0.49	5.73	3.53	4.03	0.120	0.19	0.07
SW-27 weathering rind	0.21	0.248	0.17	0.84	0.14	72.94	11.51	2.44	0.74	2.03	3.79	4.27	0.120	0.73	0.11
SW-27 rock interior	< 0.01	< 0.001	0.08	0.11	0.10	75.63	13.14	2.51	0.14	0.51	4.30	4.75	0.160	0.27	0.09
SW-50 rock interior	0.14	0.005	0.16	0.35	0.20	71.61	14.79	2.79	0.31	1.34	4.23	5.45	0.310	0.42	0.11
SW-50 weathering rind	0.56	< 0.001	0.23	0.24	0.25	72.36	14.04	2.55	0.37	1.90	4.16	5.10	0.300	0.26	0.10
SW-50 weathering rind															

S % (Leco)	FeO %	+H2O %	-H2O %	SiO2 %	Al2O3 %	Fe2O3 %	MgO %	CaO %	Na2O %	K2O %	TiO2 %	P2O5 %	MnO %
BH-13 coating	0.028	2.78 not/ss	0.21	51.67	24.23	6.32	1.68	3.12	4.32	4.26	1.250	0.43	0.66
BH-60 coating	0.023	1.01 not/ss	0.58	62.13	16.25	5.30	0.40	0.64	4.24	5.16	0.370	0.11	1.06
KS-10 coating	0.018	0.61 not/ss	not/ss	70.37	13.45	2.04	0.61	0.59	3.74	4.31	0.340	0.15	0.52
KS-21 coating	0.012	3.59 not/ss	0.60	46.23	15.06	12.80	6.39	6.10	2.18	1.65	2.210	1.27	1.15
SW-12 coating	0.007	3.98 not/ss	0.12	42.89	25.76	10.34	3.17	6.09	2.68	1.99	2.200	0.40	0.63
SW-20 coating	0.025	0.79 not/ss	0.30	66.29	17.22	2.70	0.33	0.92	3.53	5.12	0.390	0.11	0.65
SW-20 underetng	0.008	0.27 not/ss	0.33	70.43	14.30	2.42	0.43	0.84	3.95	5.89	0.330	0.07	0.18
SW-35 coating	0.022	0.41 not/ss	0.24	51.84	34.48	1.32	0.20	0.73	1.02	7.14	0.800	0.44	0.36
SW-50 coating	0.012	1.01 not/ss	0.20	54.49	27.74	3.24	0.29	0.72	3.14	5.07	0.580	0.10	0.57

ONE ARE PERFORMED OR SUPERVISED BY B.C. CERTIFIED ASSAYERS

CERTIFICATION:

TABLE 2. ICP analyses of coatings, weathering cortices,
and rock interiors.

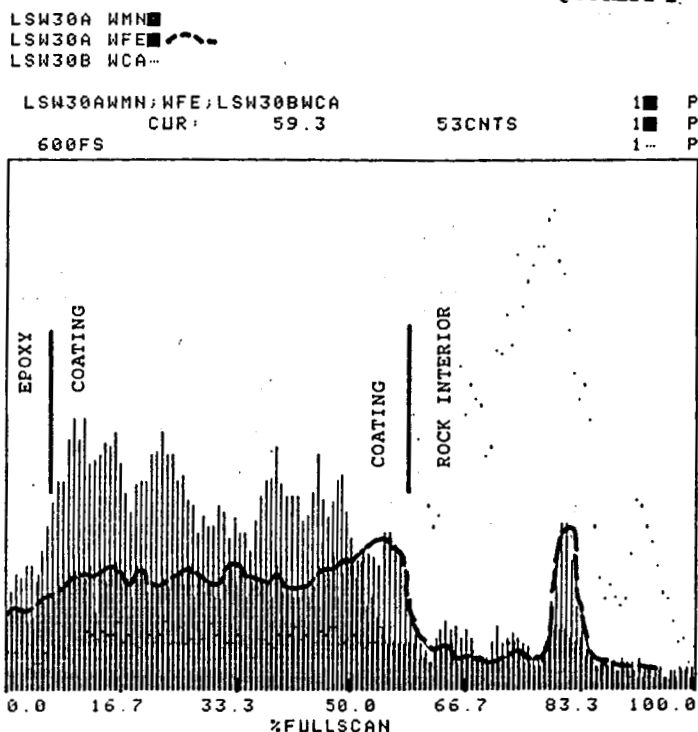


FIGURE 12. SEM line scan across coating on Spearhead Tuff from Stonewall Mountain, showing Mn lamination and relatively constant Fe, with higher Fe/Mn ratios at the rock boundary.

LKS38A WMN
LKS38A WFE

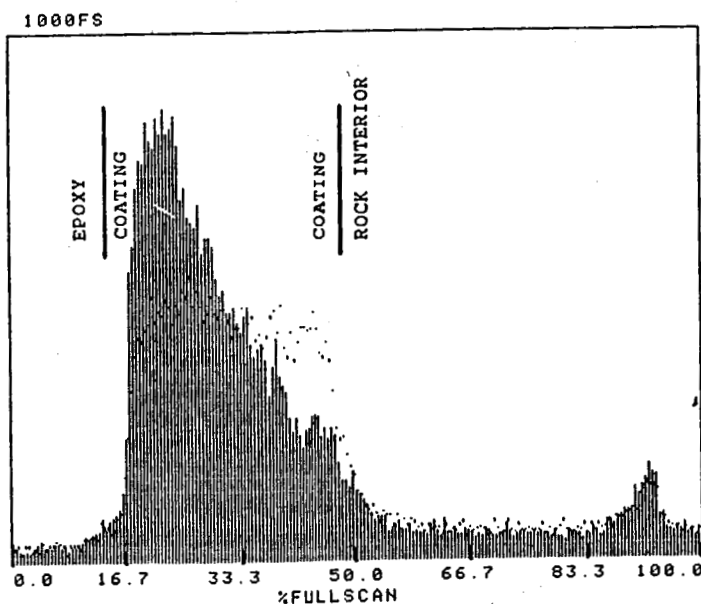


FIGURE 13. SEM line scan across coating of ash flow tuff from Kane Springs Wash, showing high Mn concentration near the outer coating edge, then tapering off with depth as the Fe/Mn ratio increases.

value between 20 and 30 (Figure 14) indicates an amorphous opaline like compound. Two samples of coatings from older tuffs from Kane Springs Wash registered a 2 theta peak near a 2d spacing for the clay mineral illite, but lacked most peaks characteristic of illite at other 2d spacings. The sample was run on the school's new Phillips XRG 3100 computerized XRD and compared with it's disc powder file library. The only realistic mineral selected was a hydrous silicate - $H_2Si_2O_5 \cdot H_2O$. It is likely the mineral is either a poorly ordered mixed-layer illitic clay or perhaps this hydrous silicate. Kaolinite is present in 2 coating samples from Stonewall Mountain - rhyolite and Andesite. No clays registered from coatings on the ash flow units. Analcime was detected in the coating sample from a minor air fall tuff unit at Stonewall. These minerals do not appear to be from the coatings themselves but rather from the rock below.

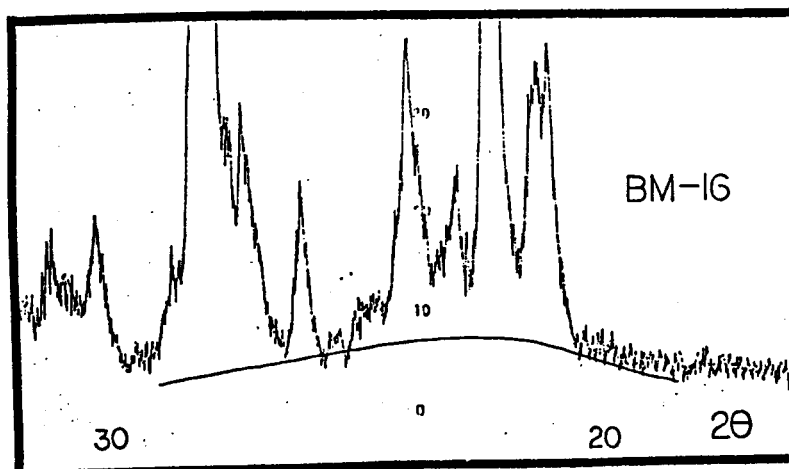
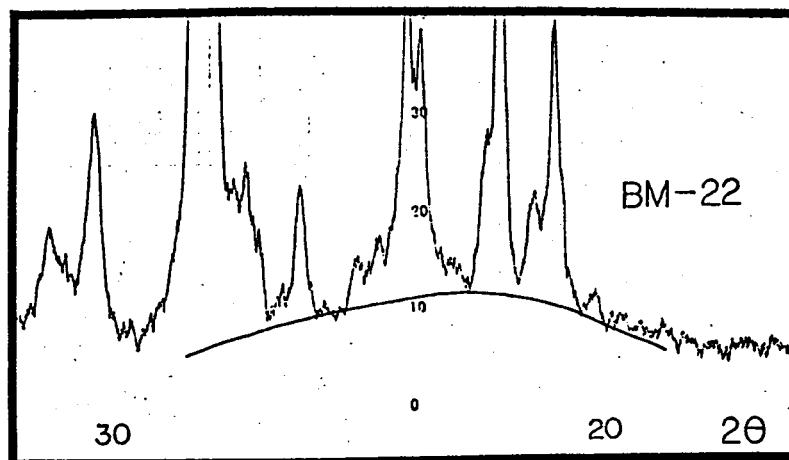
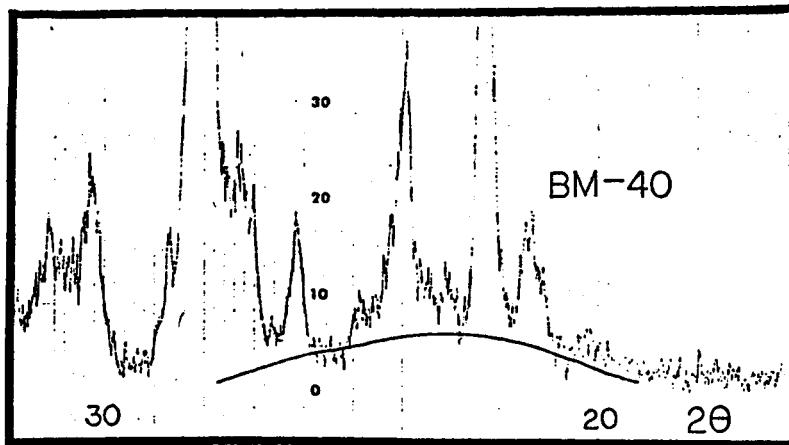
IR spectrophotometry scans of coatings (Figure 15) do not reveal any mineral phases indigenous to coatings. A broad absorption zone between about 4 and 8 micrometers indicates amorphous compounds. Variations in the water absorption peak at 6 micrometers indicates a variable hydrous component in the coatings.

ORIGIN OF THE COATINGS

The following discussion reviews the analytical results obtained from the coatings and underlying rocks and the possible geochemical environments under which they formed. Speculation on genetic models is also presented to provide a framework for further consideration.

Source of coating constituents is not understood, but most investigators believe the source is wind blown dust exogenous to the underlying host rock. The source of the Fe and Mn in the coatings must ULTIMATLY be Fe and Mn bearing minerals. The primary source of wind blown dust that comes to rest on the rock surfaces is the very rocks themselves, a conclusion Elvidge (1979) came to as well, after considering alternative sources, including present day volcanic expulsion. It is likely, therefore, that the source of the Fe and Mn in the coatings is the rocks upon which they lie or rocks within the immediate vicinity. We have investigated the substrate below the coatings including the weathering rinds and the dark weathering bands they contain as well as the coatings themselves to probe a possible genetic connection.

From field observation, we know that mineral coatings and varnish are indeed products of the weathering environment. From considerations on the



XRD

FIGURE 14. X-ray diffraction curves of samples of coatings, showing an "opaline" hump (dark line), probably generated by amorphous compounds.

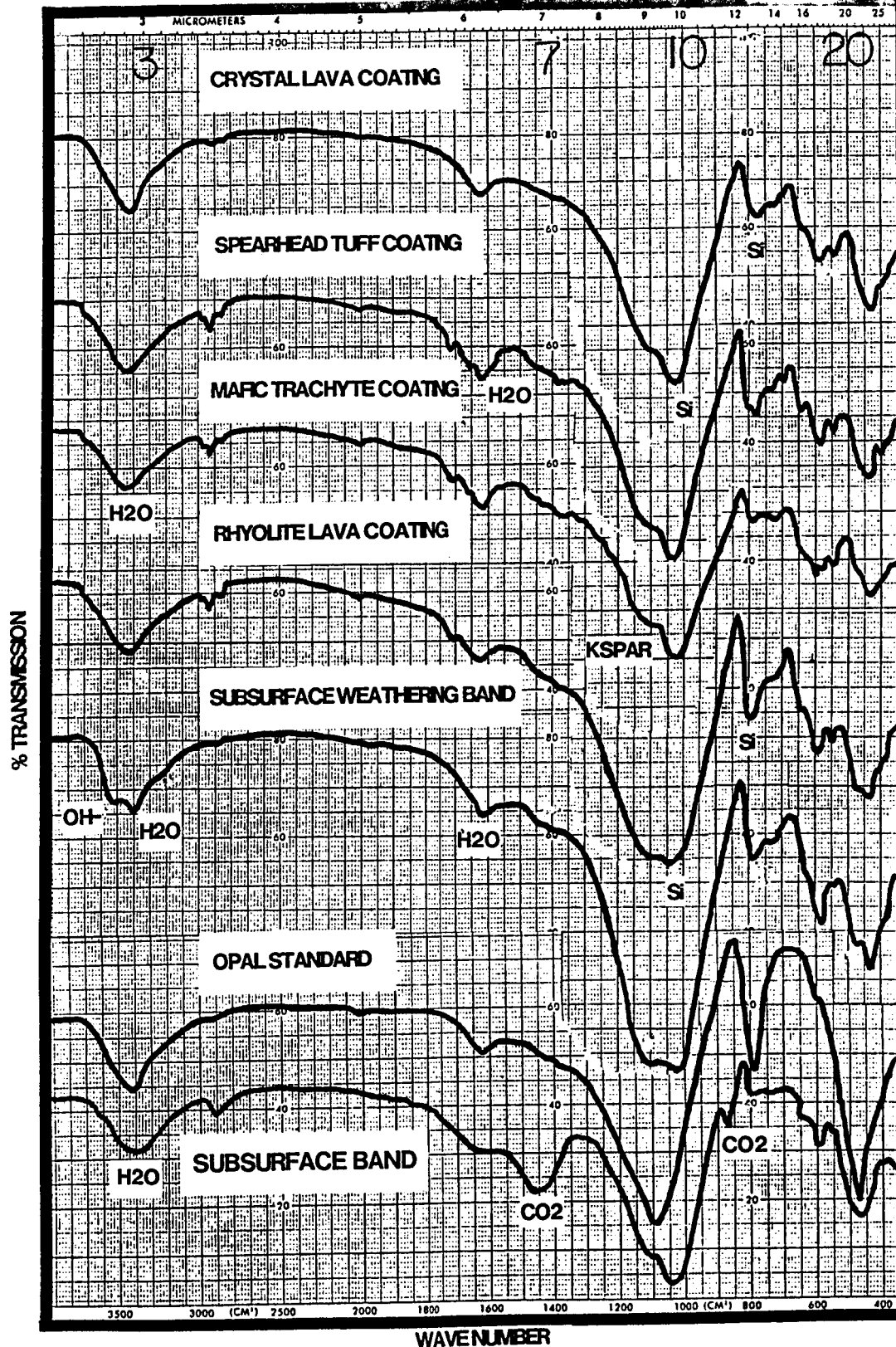


FIGURE 15. Infrared (IR) spectrophotometry scans of coatings and other material.

ORIGINAL PAGE IS
OF POOR QUALITY

geochemistry of natural waters, Fe, and Mn, we can establish a likely geochemical environment within which the relationships we observe make sense. Important considerations will include pH, Eh, and dissolved ions. We assume from our study that coatings are amorphous compounds or poorly ordered hydroxides of Mn, Fe, Si, and Al.

IRON AND MANGANESE

Figure 16 shows Eh-pH relationships for both Fe and Mn. Under moderately oxidizing conditions, both Fe and Mn are soluble below a pH of about 6, but form oxides and hydroxides at higher alkalinities. Noncrystalline phases are favored by rapid precipitation which we might expect on the surface of rocks in semi-arid environments where dissolution and precipitation may follow pH fluxuations after rain showers. Mn is more mobile than Fe and thus precipitates more slowly. Mn can remain soluble in aerated waters at pH values in excess of 9.0, whereas Fe would be likely precipitated (Hem, 1964). This could account for the observed concentration of Mn relative to Fe at the outer coating surface and its concentration in layers within the coatings possibly recording climatic cycles involving either humidity or temperature (cooler climates would favor increased CO₂ concentration, prolonged acidic conditions, and greater dissolution and concentration of Mn.)

Carbon dioxide as undissociated carbonic acid, bicarbonate and carbonate ion is the pH buffer of most natural waters (Hem, 1960). The atmosphere contains about 0.03 percent CO₂ by volume, but plants contribute further by respiration and decay. (According to Hem, only a small proportion of CO₂ dissolved in water forms carbonic acid.) Thus rain water, falling and collecting on the surface of the volcanic rocks in southern Nevada, would likely be enriched in CO₂ from the lichen and other organics growing on the rocks. The acidic environment around lichen is supported by the general lack of coatings around lichen; however, Oborn (1960) mentions that crustose lichen metabolize Fe and remove it from the rock. These relationships are further obscured by the fact that lichen often favor poorly welded, vapor phase altered tuffs, which do not typically develop mature coatings anyway. Coatings tend to accumulate in the recesses of rocks where water would drain, collect, and reside the longest.

Hem (1963) found that precipitates of Mn formed at pH values between 8 and 9 contained too little Mn to be Mn oxides suggesting that the precipitates contained water. He speculated that the solid phase was likely Mn(OH)₃. Hydrous precipitates of both Fe and Mn lose

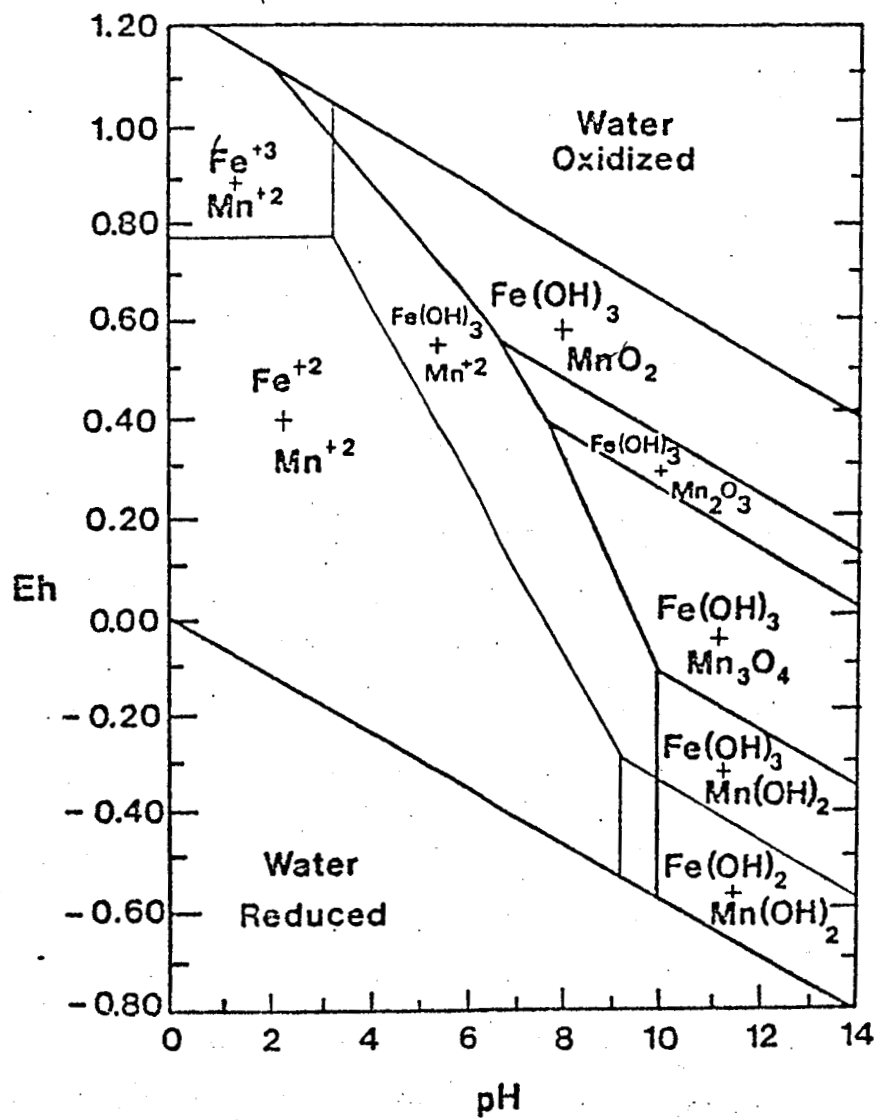


FIGURE 16. Eh-pH graph, showing stability fields for different Mn and Fe species.

water and grow increasingly less soluble with time. Johnston and Lewis (1983) found that with time ferrihydrite converts to hematite by particle coalescing.

WEATHERED CORTEX. A weathering rind develops on all the volcanic rock types studied. It is a 0.3 - 15mm thick plate that exfoliates outcrop surfaces and spalls off carrying the coatings with it. Table 2 compares major element analyses of the rinds with their parent rocks. Rinds are enriched in CO₂ relative to interiors on the tuffs but not relative to the dense rhyolites or basalts. Rinds tend to contain more S and both essential and nonessential H₂O. Rinds appear depleted in SiO₂ relative to underlying interiors. For the most part rinds show some apparent depletion in Al₂O₃ especially for the more porous tuffs. For most cases there is a slight depletion in total Fe, reported as Fe₂O₃ in the rinds. The major exceptions are basalt from Kane Springs Wash (KS-21) and other mafic units. MgO and CaO are enriched in rinds. MnO shows if anything a slight enrichment in the rinds. As will be discussed later, SEM probes indicate some geochemical stratification within the weathered cortex itself.

From thin sections and application of hydrochloric acid to hand samples we know that the rinds contain carbonate which would account for their enrichment in CaO, MgO, and CO₂. The higher H₂O content of the rinds indicates hydration, and apparent depletion in alkalis and iron suggest leaching. The rinds are weathered cortexes and reflect geochemical interaction with the weathering environment. The extent to which they may relate to coatings will be discussed below.

SEM probes of the dark bands that occur within the weathered cortex are tabulated in Table 1. Compositions of the bands are similar those of the weathering cortex. Enrichment in CaO is the only consistent compositional difference between the secondary band and the enclosing weathering cortex. From thin section petrography we know that some of the bands are distinctly carbonate rich. Zeolites have been tentatively identified, but the association may be fortuitous. Secondary SEM X-rays reveal that the bands are dense, less porous, and evidently zones of cementation. They appear harder to a knife blade as well. The bands seem to contain a distinct hydrous component (IR spectra, Figure), and they appear cloudy in thin section suggesting presence of an amorphous compound, perhaps similar to the coatings.

Analcime was detected by XRD in a porous air fall tuff from Stonewall Mountain. The occurrence of zeolites in tuffaceous rocks is well documented

(Mumpton, edit., 1977). The origin of analcime, a Na bearing zeolite, commonly in association with alkaline rocks like those in the project areas, is not understood (Hay, 1977) but reaction with meteoric waters is one hypothesis. Reaction of glass to zeolites seems unequivocal (Hay and Sheppard, 1977). Deffeyes (1959) and Mumpton (1973) have shown that the reaction involves diagenetic solutioning of glass, then precipitation of zeolites rather than formation through divitrification. According to Mariner and Surdam (1970), an aluminosilicate gel may first form from the glass, from which zeolites grow. This relationship could account for the apparent association of zeolites with amorphous compounds in the weathering bands described earlier. Zeolites are preferred over clays because of the cation/hydrogen ratio. Cations excluded from the zeolite structure could remain in solution for transport to other sites.

The carbonate mineralization which seems to correlate directly with tuff porosities and to concentrate in the weathered cortex resembles caliche zones and may follow principles of caliche formation. Aridic soils, in contrast to humic soils, are characterized by concentrations of calcium salts somewhere in their profile (Krauskopf, 1967). Rain water soaks into the soil and porous rocks, as well, and later is pumped back toward the surface by capillary action. Only the most soluble cations would be leached. Namely, Na, K, and Mg. Calcium would largely remain behind in a layer that represents a solution front. The distinct, dark bands may reflect the lower edge of the solution front's advance into the tuffs. They are enriched in Ca, and for some of the more porous tuffs (BM-46 and KS-57, Table 1) the rock zone just above is slightly enriched in sodium.

SOURCE OF Mn AND Fe. We have looked at coating distributions on the rock surfaces from optical, SEM, and density slice methods and found that the amount of encrusting varnish 3-20 micrometers thick, rarely up to 50 micrometers thick, is greatly subordinated by thin films which coat the surface, and impregnate the rock intergranularly, rarely up to 0.5 mm depths, without discernable build-up. For this reason the ICP analyses of coatings (Table 2) record a maximum of only 1.15% MnO. These samples were extracted from the rock by a carbide scribe moved lightly over the surface. Samples were screened to -100 mesh to reduce contamination by extraneous mineral grains. Binocular scope optical examinations indicate that the samples represent depths averaging about 0.20mm thick and rarely includes material below 0.5mm. From these data we can evaluate the rock substrate, particularly the weathered cortex, as a potential source of Mn and Fe.

The coating sample from Civet Cat Canyon Tuff (Table 2, SW-20) contained 0.65% MnO with underlying Civet Cat reporting 0.10%. Basalt (KS-21) coatings contained 1.15% MnO, the underlying rock - 0.12%. Using an estimated density for densely welded Civet Cat of 2.3 and a density of 2.5 for its coating, the estimated volumetric amount of Mn in the coating is 0.0163 gms/cm³ with 0.0023 gms/cm³ in the underlying rock, a 7.1 enrichment factor. Since the coating sample was less than 0.5mm thick we can estimate roughly that 7 times the same thickness would represent the amount of underlying column that would contain an equal amount of MnO. That depth is about 3.5 mm. If only 25% of the Mn were extracted from a near surface zone of leaching, a 14mm thick weathering cortex would be required, which is well within typical thicknesses of weathering zones observed on many of the tuffs. Since the actual coating sample thickness was probably closer to 0.25 than 0.5mm, only a 7mm thickness would be required, or to look at it another way, only 13% or so of the Mn would have to be leached from a 14mm deep column. SEM probes of olivine in mafic trachyte and aegerine in the Gold Flat Tuff (Table 1) show MnO contents of 1.91% and 1.21%, respectively, likely sources of the Mn even if from wind blown dust.

Similar calculations for the basalt indicate a 9.6 enrichment factor in the coating sample (including the 0.25mm substrate). So leach extraction depths of 2.4mm would be required if all Mn originated from the substrate; or 12mm if leaching efficiency were only 20%.

Similar relationships bear for Fe. In the case of Fe, reference to Table 2 shows some evidence that the weathering rinds are depleted relative to the underlying rock. One major exception is the basalt (KS-21). Mn appears significantly depleted in the subsurface zones of samples BM-46, KS-57, and SW-30 probed with the SEM (Table 1) relative to deeper zones within the rock. Mn on the other hand shows no depletion zone in the ICP data, but since we are dealing with such small amounts (typically 0.15% or so) further analytical work might be warranted.

GEOCHEMICAL MODELS FOR COATING FORMATION

This is an interim report. This discussion of possible genetic models is thus preliminary and intended to stimulate discussion. Final conclusions will not be drawn until the final report.

The zoning and ion concentration relationships observed in the data presented above support a leaching process in the weathered cortex of volcanic rocks at

the study sites much like the solution front system described by Krauskopf (1967) for caliche formation in aridic soils. A slightly acidic carbon dioxide and carbonic acid enriched solution created from atmospheric interaction and biogenic processes at the rock's surface would soak into the surface, permeating the porous tuffs to a greater extent than the more dense flows. Carbonate rich cortices and dark hydration bands develop near the lowest extent of solution front advance where Mg rich calcite and amorphous, opaline deposits precipitate out of a solution supersaturated in these components as a function of leaching the overlying substrate (the CO₂ was already present in the leachant) and evapotranspiration of water moving by capillary action back out of the rock. More soluble components remain in the retreating solution and are precipitated when supersaturation levels are reached as the solution regresses toward the rock surface. Na, for example, appears to concentrate in the upper part of the weathered cortex.

The banding relationships in layered desert varnish and the Fe/Mn ratio of coatings may be explained in context of this solution pump. Mn tends to concentrate at the outer edge of the varnish and to form concentrated layers within some of the varnishes at lower levels. The Fe/Mn ratio generally increases toward the lower edge of the coatings and Fe is sometimes concentrated in a layer at the rock interface. This relationship seems reverse to that which one might expect if all the Fe and Mn were leached from surficial dust, since Mn is the more soluble and mobile of the two elements. If Mn and Fe were contained in a solution that was undergoing extraction out of the rock by evapotranspiration, Fe might be expected to precipitate at the air interface in response to higher Eh conditions, possibly forming a poorly crystalline ferrihydrite phase which some workers feel could be a coating component (Johnston and Lewis, 1983). Mn would remain in solution longer and precipitate out at the coating air interface in response to evaporation and supersaturation.

Another explanation for the high Mn zone at the coating surface could be successive resolutioning and redeposition of the relatively mobile metal; however, one might expect more dispersion in this case and Mn distribution to greater depths, like Fe. Another reason for Mn concentration at the surface which other workers have suggested is microbial fixation, possibly ubiquitous bacterial activity.

Some correlation between underlying host rock and coatings and a possible genetic link is indicated by differences in Fe and Mn relationships between the more

mafic units and the more felsic deposits. Basalt coatings (KS-21 and SW-12) exhibit a higher Fe/Mn ratio than coatings from more felsic rocks and higher overall Fe and Mn content as well. This suggests an underlying host rock origin rather than exogenous wind blown dust from other units; however, it does not preclude dust which originated from the basalt itself.

These possible genetic mechanisms for coating formation will be investigated in more detail in the months to come as more data is collected.

INFLUENCE OF MINERAL COATINGS ON TM IMAGERY

Early attempts to describe mineral coatings in desert environments (desert varnish) in a comprehensive fashion were published by White (1924), Laudermilk (1931), and Engel and Sharp (1958). A more quantitative approach to the study of coatings began in the mid-1970's and numerous workers have published their results since. Dorn and Oberlander (1981) in a fairly lengthy treatise on the topic do an excellent job of summarizing work on coatings up to that time.

Desert varnish is usually defined as the arid secondary phase at the weathered surface of rocks in arid to semi-arid environments. To most field geologists in the U.S. desert varnish is that conspicuous dark rusty brown to shiny black stain that commonly coats prominent bluffs in our semi-arid Southwest. Iron and manganese oxides are the distinctive components. For purposes of remote sensing, we are concerned with the entire surface of a rock exposure, which may include both true desert varnish, subvarnish alteration zones, and relatively fresh rock. Any given scene typically contains a combination of rock surface types. Previous workers have diverged on source of varnish constituents. Engle and Sharp (1958) concluded that the components of desert varnish are derived from the underlying host rock, whereas Dorn and Oberlander (1981) state flatly that the constituents are derived from external sources. The proponents of an external source point to wind blown dust as the feedstock. In this section we review the coating characteristics presented above to the extent which they may influence remote sensing data.

Coatings are characteristically thin and discontinuous. They are a reddish brown to dark brown amorphous mass that tends to coat mineral grains at the surface and penetrate as a thin film intergranularly up to 1-1.5mm into the rock. SEM scans reveal that the thickest surface deposits rarely exceed 20-30 micrometers and that even a well coated surface is dominated by much thinner films of coating. The thick,

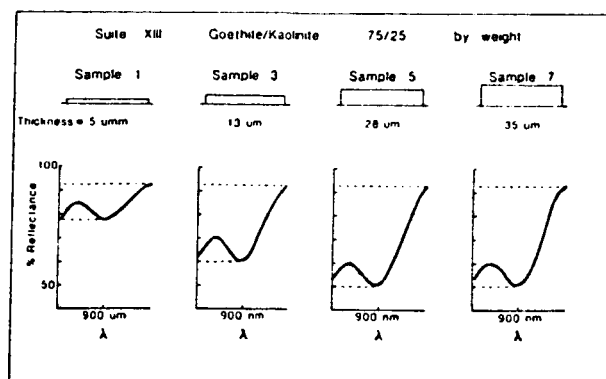
20-30 micrometer deposits are sporadic and discontinuous, concentrated in small protected recesses.

Major element compositions (SEM analyses) of coatings from rock surfaces of all rock types from each area, including quartzite from Stonewall Mountain, are quite similar - about 45-60% Fe and Mn and 40-50% Si and Al - an observation important to remote sensing efforts. Either Mn or Fe alone can exceed 30%. Except for Fe/Mn ratios on basaltic rocks tending to be higher than on other units, there does not appear to be any distinctive correlation between coating compositions and host rock lithology. No significant amount of clay minerals or other crystalline compounds have yet been detected, either from thin section observation, X-ray powder diffraction, or IR spectral scans. (Detail on compositions, distributions, and relationship of coatings to underlying rock is the subject of a paper in preparation by the authors and Jim Sjöberg of the U.S. Bureau of Mines).

Coatings develop to an advanced stage of maturity only where the surface is resistant and durable. Surfaces do not exhibit significant coating continuity. Where coated surfaces become breached by weathering or where deposits have not matured to an advanced state, relatively fresh rock is exposed. Over any given surface about 4x4 meters or so square, significant varnish rarely accounts for over 50% of the exposure. Removal of coated surfaces is expedited by development of weathering rinds, .25-2.0 cm thick, which spall off outcrop surfaces. It is this process that leads to case hardening and exfoliation.

Figure 4 shows a gray level slice from a varnished rock surface computed with a Dapple optical image analysis system. The coating is moderately well developed on this sample, and density slicing was controlled to segregate relatively fresh rock exposure from coated surface. Note that the coated surface accounts for only 37% of the exposure. The importance of coating to the overall spectral composition seems further reduced by field and thin section observation and SEM scans that indicate that the great majority of coated surfaces are discontinuous and that build-up of encrusting coatings or varnish is sparse.

Penetration of electromagnetic energy within the TM range was studied by Buckingham and Sommer (1983) who found that maximum penetration for pulverized samples of clay minerals was about 50 micrometers (Figure 17). A mixture of goethite and kaolinite - 75/25 - stopped penetration of 0.8 - 1.0 micrometer wavelengths at around 25-30 micrometers.



Absorption vs Sample Thickness

0.9 Micrometers

W.F. Buckingham and S.E. Sommer, 1983

FIGURE 17. Effect of sample thickness (geothite/kaolinite mix) on absorption at 0.9 micrometers.

Amorphous, translucent compounds like those that make up the coatings of this study would transmit light further than crystalline mixtures of iron oxide and clays. In other words, light would penetrate in part (increasingly with increasing wavelengths) completely through even the thickest concentrations of coatings yet discovered in this study reflecting to at least some degree the primary character of underlying rock to the extent that it is unaltered.

The effect of coatings on the spectral response of volcanic unit in the project areas to the TM range is shown in Figure . Coated surfaces are compared to uncoated but somewhat weathered surfaces. Note that shorter wavelengths are absorbed by coatings to a greater extent than longer wavelengths. Beyond about 0.7 - 1.3 micrometers, depending on mafic affinity of the host rock, reflectance becomes less dependent on coatings for some units. In the case of the sample of Gold Flat Tuff, coatings tend to simply diminish reflectance throughout the TM interval. (A similar relationship was reported by Farr, 1981.) The basalt, mafic trachyte, and ash flow tuff (dark, ferruginous Civet Cat) samples show the typical absorption of coatings in the lower wavelength interval, but actually record higher reflectance beyond 0.7 to 1.3 micrometers for the coated samples. This relationship appears due

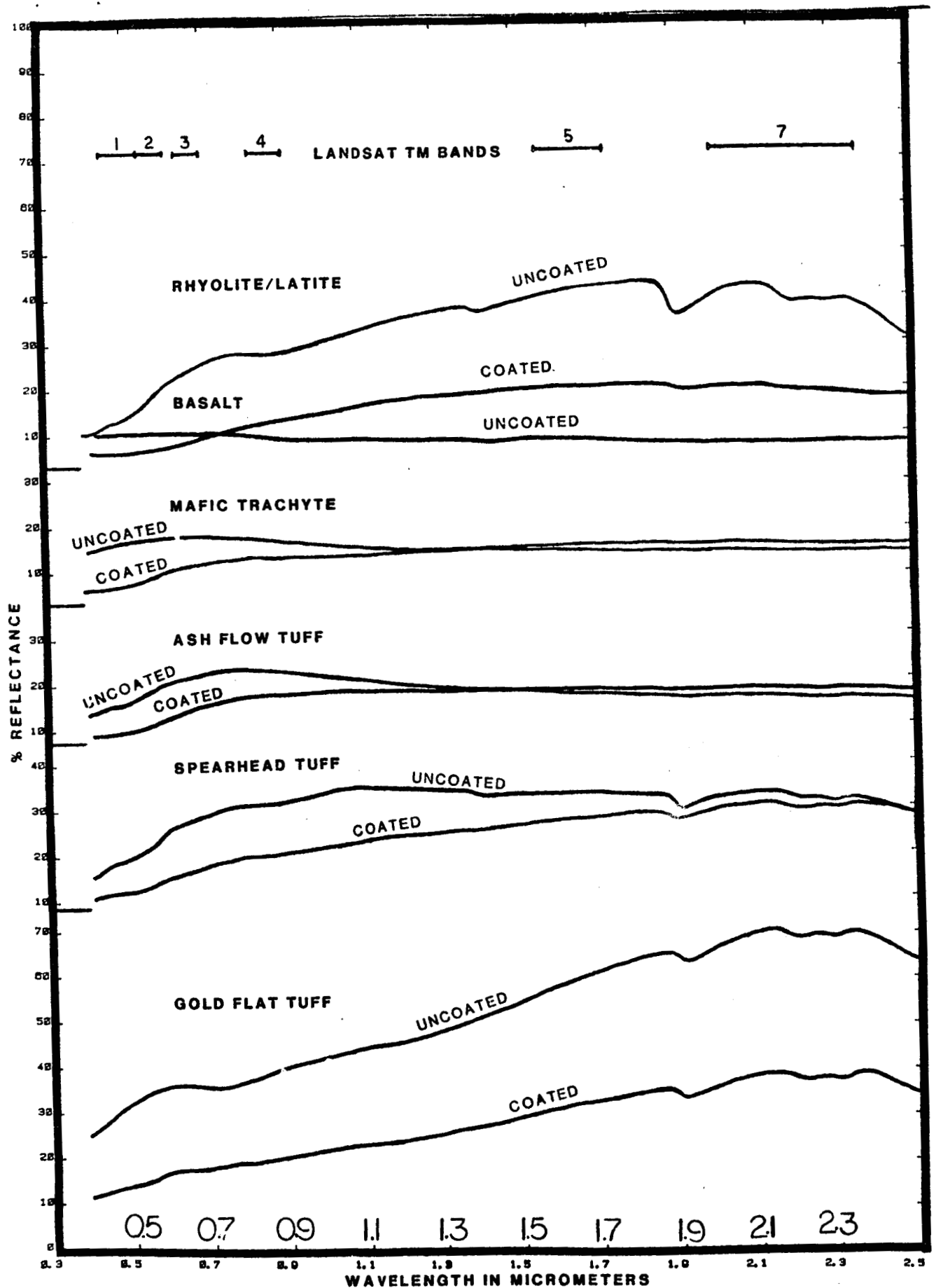


FIGURE 18. Spectral curves for coated rock surfaces compared to their uncoated counterparts (only an uncoated sample shown for the rhyolite/latite sample).

to the relatively higher absorption and low albedo of fresh melanocratic rocks relative to coatings which consist of amorphous translucent compounds high in Si and Al. This relationship seems supported by the general tendency for reflectance to increase with an increase in wave number for coated samples, but decrease or level off for the uncoated samples. Thus a band 5/7 ratio would tend to decrease the DN values of coated samples relative to uncoated ones.

CONCLUSIONS

Laboratory spectral comparisons suggest that coatings are relatively unimportant to the overall spectral character of volcanic rocks in the longer wavelength TM interval. This conclusion seems consistent with observations that coatings are relatively thin, amorphous, translucent, and less absorptive to wavelengths of about 0.7 micrometer and longer. The significance of coatings and varnish to reflectance imagery is further reduced when one takes into account that varnished rock typically makes up only a small portion of any pixel-sized scene and that coatings on an exposure of relatively mature varnish is incomplete. The absorptive properties of coatings in the shorter wavelength intervals should provide a spectral distinction - dark tonal contrast - in bands 1 and 2. Coated surfaces should darken in tonal contrast in a band 5/7 ratio since reflectance of coated surfaces tends to increase throughout this range, whereas reflectance decreases on uncoated surfaces.

Contrast enhanced composite TM images of longer wavelength bands, particularly bands 3, 5, and 7 and composite images of these three bands in contrast enhanced mode (scaled), provide striking lithologic contrast between some of the volcanic flows at the Black Mountain caldera. Concentration of vegetation is mapped by the 4/3 ratio image, which is mirrored on the PC3 image. Since some formations are uniquely exhibited in color contrast on some images, yet bear diverse vegetative canopies, it is concluded that the unique color contrast is more a result of lithologic spectral response than a vegetative or mineral coating control. The longer wavelength bands (bands 5 and 7 especially), PC 2, and intensity and hue images of bands 3, 5, and 7 isolate reflective spectral contrast between lithologic units at the Black Mountain caldera.

REFERENCES

- Allen, C.C., 1978, Desert varnish of the Sonoran Desert: optical and electron probe microanalyses: Jour. of Geol., v.86, p. 743-752.
- Berner, R.A., and Holdren, G.R., Jr., 1977, Mechanism of feldspar weathering: some observational evidence: Geology, v.5, p.369-372.
- Borns, D.J., Adams, J.B., Curtiss, B., Farr, T., Palmer, F., Staley, J., and Taylor-George, S., 1980, The role of micro-organisms in the formation of desert varnish and other rock coatings: SEM study: GSA Abst., v.12, p.390.
- Clark, S.P., 1957, Absorption spectra of some silicates in the visible and near infrared: Amer. Mineralogist, v.42, p.732-741.
- Curtiss, B., Adams, J.B., and Ghiorso, M.S., 1985, Origin, development and chemistry of silica-alumina rock coatings from the semi-arid region of the Island of Hawaii: Geoch. Et Cosmo Chem. Acta, Jan. vol.
- Deffeyes, K.S., 1959, Zeolites in sedimentary rocks: J. Petrol., v.29, pp 602-609.
- Dorn, R.I. and Oberlander, T.M., 1981, Microbial origin of desert varnish: Science, v. 213, p. 1245-1247.
- Dorn, R.I. and Oberlander, T.M., 1982, Rock varnish: Prog. in Phys. Geog., v.6, p.317-367.
- Elvidge, C., 1979, Distribution and formation of desert varnish in Arizona (MS Thesis): Tempe, Ariz., Arizona State Univ., 109 p.
- Engel, C.G. and Sharp, R.P., 1958, Chemical data on desert varnish: GSA Bull., v.69, p.487-518.
- Farr, T.G., 1981, Surface weathering of rocks in semiarid regions and its importance for geologic remote sensing (Ph.D. thesis): Seattle, Wash., Univ. of Washington, 149 p.
- Farr, T.G. and Adams, J.B., 1984, Rock coatings in Hawaii: GSA Bull., v.95, p.1077-1083.
- Glasby, G.P., McPherson, J.G., Kohn, B.P., Johnston, J.H., Keys, J.R., Freeman, A.G., and Tricker, M.J., 1981, desert varnish in Southern Victoria Land, Antarctica: New Zealand Jour. of Geol. and Geoph., v.24, p.389-397.

Hay, R.L., 1977, Geology of zeolites in sedimentary rocks IN Mumpton, F.A. edit. Mineralogy and geology of natural zeolites: Miner.Soc.Amer.short course notes, v.4, pp53-64.

Hay, R.L. and Sheppard, R.A., 1977, Zeolites in open hydrologic systems IN Mumpton, F.A. edit. Mineralogy and geology of natural zeolites: Miner.Soc.Amer.Short course notes, v.4, pp 93-102.

Hem, J.D. and Cropper, W.H., 1959, Survey of ferrous-ferric chemical equilibria and redox potentials; U.S.G.S. water supply pap.1459-A, 30p.

Hem, J.D., 1960, Restraints on dissolved ferrous iron imposed by bicarbonate redox potential, and pH: U.S.G.S. water supply pap.1459-B, p33-55.

Hem, J.D., 1963, Chemical equilibria and rates of manganese oxidation: U.S.G.S. water supply pap.1667-A, 64p.

Hem, J.D., 1964, Deposition and solution of manganese oxides: U.S.G.S. water supply pap.1667-B, 42p.

Hooke, R.LeB., Yang, H., and Weiblen, P.W., 1969, Desert varnish: an electron probe study: Jour. of Geol., v.77, p.275-288.

Hunt, C.B., 1954, Desert varnish: Science, v.120, p.183-184.

Hunt, C.B., 1961, Stratigraphy of desert varnish: U.S.G.S. Prof.P.424-B, p.194-195.

Johnston, J.H. and Lewis, D.G., 1983, A detailed study of the transformation of ferrihydrite to hematite in an aqueous medium at 92 degrees C: Geoch. et Cosmochem.Acta, v.47, pp1823-1831.

Keller, W.D., 1977, Scan electron micrographs of kaolins collected from diverse environments of origin: Clays and Clay Mineralogy, v.25, p.347-364.

Knauss, K.G. and Ku, T., 1980, Desert varnish: potential for age dating via uranium-series isotopes: Jour. of Geol., v.88, p.95-100.

Krauskopf, K.B., 1967, Introduction to geochemistry: McGraw-Hill Book Co., New York, N.Y., 721p.

Krumbein, W.E. and Jens, K., 1981, Biogenic rock varnishes of the Negev Desert (Israel): an ecological study of iron and manganese transformation by

cyanobacteria and fungi: *Oecologia* (Berl.), v.50, p.25-38.

Laudermilk, J.D., 1931, On the origin of desert varnish: *Amer. Jour. of Science*, v.21, p.51-66.

Mariner, R.H. and Surdam, R.C., 1970, Alkalinity and formation of zeolites in saline alkaline lakes: *Science* v.170, pp977-980.

Mumpton, F.A., 1973, Scanning electron microscopy and the origin of sedimentary zeolites: *Molecular sieves, Proc.3rd Int.Cont.Mol.Sieves*, Uytterhoeven, J.B., edit., Leuven Univ.Press, pp56-61.

Mumpton, F.A., edit., 1977, Mineralogy and geology of natural zeolites: *Miner.Soc.Amer.short course notes*, v.4, 233p.

Osborn, E.T. and Hem, J.D., 1961, Microbiological factors in the solution and transport of iron: *U.S.G.S. water supply pap.1459-H*, pp 213-235.

Perry, R.S. and Adams, J.B., 1978, Desert varnish: evidence for cyclic deposition of manganese: *Nature*, v.276, p.489-491.

Potter, R.M. and Rossman, G.R., 1977, Desert varnish: the importance of clay minerals: *Science*, v.196, p.1446-1448.

Potter, R.M. and Rossman, G.R., 1979, The manganese and iron oxide mineralogy of desert varnish: *Chemical Geology*, v.25, p.79-94.

Schwertmann, U. and Fischer, W.R., 1973, Natural "amorphous" ferric hydroxide: *Geoderma*, v.10, pp 237-247.

Staley, J.T., Palmer, F., and Adams, J.B., 1982, Microcolonial fungi: common inhabitants of desert rocks: *Science*, v.213, p.1093-1094.

White, C.H., 1924, Desert varnish: *Amer.Jour.Sci.*, v.7, 5th ser., p.413-420.